

Readout of Silicon Detector telescopes with a new frontend chip

A. Mussgiller, S. Barsov¹, T. Krings, I. Lehmann², V. Leontyev, S. Merzliakov³, D. Protic, R. Schleichert, S. Trusov²

The first two Spectator Telescopes have been installed at ANKE during beamtimes in August and November of 2003. Both telescopes are equipped with a $70\ \mu\text{m}$ double sided silicon strip detector and a $5.1\ \text{mm}$ thick double sided Si(Li) detector. The read out is performed by custom made electronics and the newly developed VA32TA2 frontend amplifier. This charge sensitive preamplifier chip is the combination of the VA32_HDR2 and the TA32cg discriminator chip [1]. The performance of the chips and detectors is shown on basis of data from the beamtime in August.

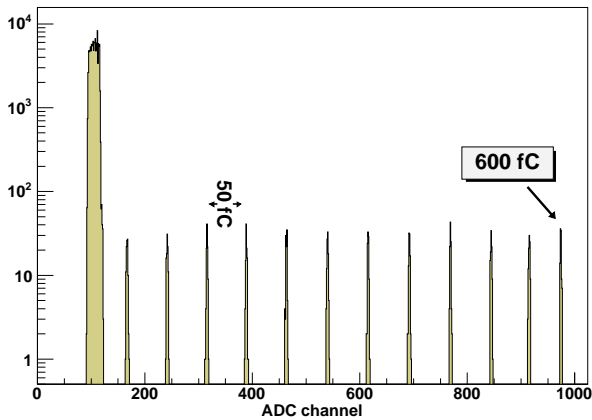


Fig. 1: Typical test pulse histogram for negative input charges

The chip houses 32 channels, each of them equipped with a slow shaper and a fast shaper with discriminator. The threshold of each discriminator can be adjusted individually to allow a common threshold for all 32 channels.

For calibration and diagnostic purposes the chip can be switched into test mode in which it is possible to inject a test charge into a selected channel by applying a voltage step over a capacitor. The test charge Q is given by $Q = C \cdot \frac{U}{3}$ with C being $1\ \text{pF}$. The factor of 3 is due to an internal division of the test voltage. Figure 1 shows a typical test pulse histogram for negative input charges. The distance between each peak is $50\ \text{fC}$ with a maximum test amplitude of $600\ \text{fC}$.

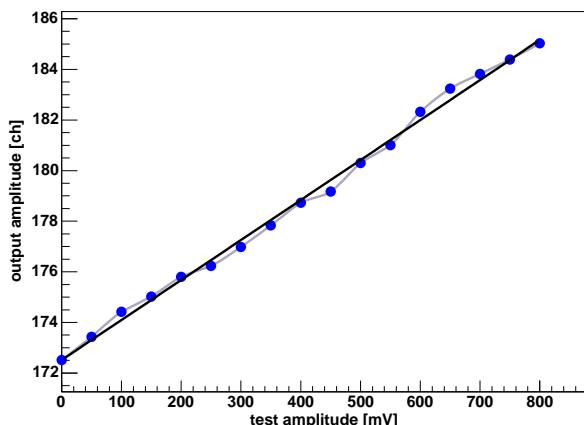


Fig. 2: Position of the pedestal as a function of the test pulse amplitude

The pedestal in the figure is not of gaussian shape but rather a flat distribution. The reason for this is a common shift of the baseline of the frontend electronics. Figure 2 in which the position of the pedestal is plotted against the amplitude of the voltage step shows this behaviour.

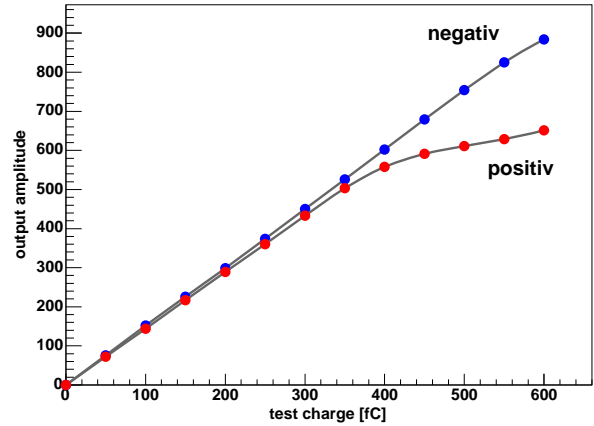


Fig. 3: Fit to the test pulse data for both positive and negative charges

In figure 3 the distance between the test pulse peak and its corresponding pedestal is plotted against the test pulse amplitude. For the applied settings and bias voltages of the chip it shows a linear behavior up to $\approx 550\ \text{fC}$ for negative charges while the linear range for positive test charges is limited to only $\approx 400\ \text{fC}$. With improved settings and bias voltages it is possible to extend the linear range for positive charges up to $\approx 500\ \text{fC}$. A 4th order polynomial fit to the data points gives a preliminary energy calibration for each channel.

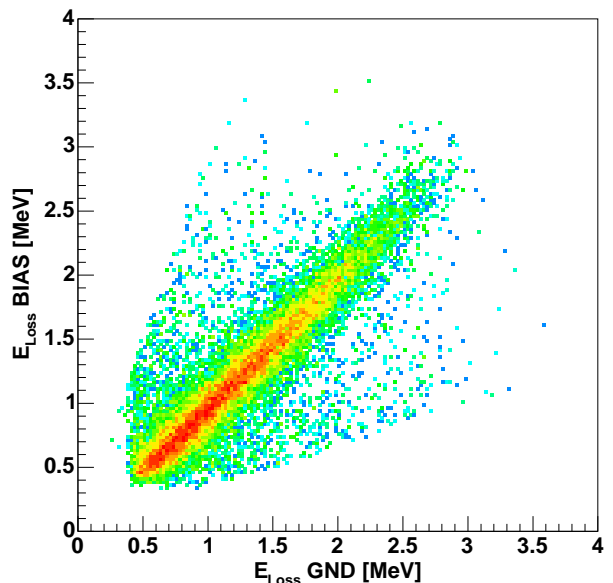


Fig. 4: Energy loss from the BIAS side vs. the energy loss of the GND side of the $70\ \mu\text{m}$ detector

The validity of the energy calibration obtained by the test pulse measurement is checked by applying it to real data.

Figure 4 displays the energy loss from the BIAS side of the $70\ \mu\text{m}$ detector versus the energy loss from the GND side of the same detector. The distribution shows equal energy losses for both sides which is a clear indication that the energy calibration compensates all non linearities. The remaining difference to the final energy calibration is a factor for each detector which is due to the difference between the effectively used test pulse capacitance and the nominal capacitance.

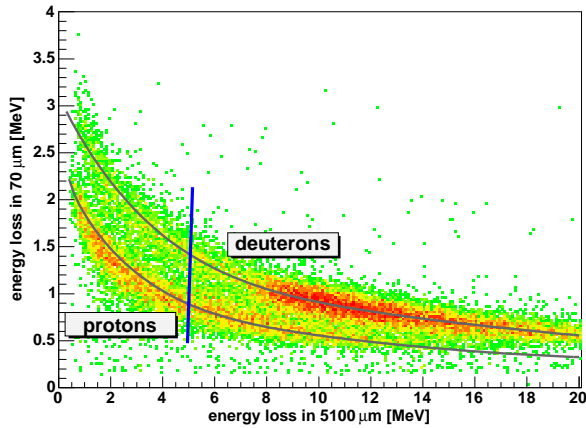


Fig. 5: Energy loss in the $70\ \mu\text{m}$ vs. the energy loss in the $5.1\ \text{mm}$ thick detector

The remaining calibration factor is obtained by utilizing the detection principle of the spectator telescope. At ANKE the telescopes are used to detector low energy protons and deuterons. To distinguish between the two particles the $\Delta E/E$ method is used. Figure 5 shows the energy loss of a particle in the first ($70\ \mu\text{m}$) versus the energy loss in the second ($5.1\ \text{mm}$) detector layer. The gray curves in the histogram indicate SRIM[2] calculations for protons and deuterons. The final calibration is obtained by fitting a sample of identified protons and deuterons to the calculated curves. Figure 5 already shows a histogram which has been produced with the final energy calibration.

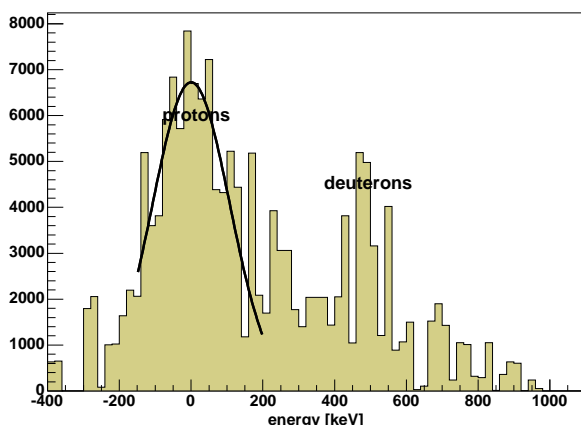


Fig. 6: A slice taken along the line indicated in blue in figure 5 results in an energy resolution of $240\ \text{keV}$

Figure 6 shows the energy resolution of the telescope which is given by a projection along the blue line indicated in figure 5. A fit around the proton peak results in an energy resolution of $240\ \text{keV}$. One of the possible reasons for the poor energy

resolution are the high detector leakage currents after a vacuum break at COSY.

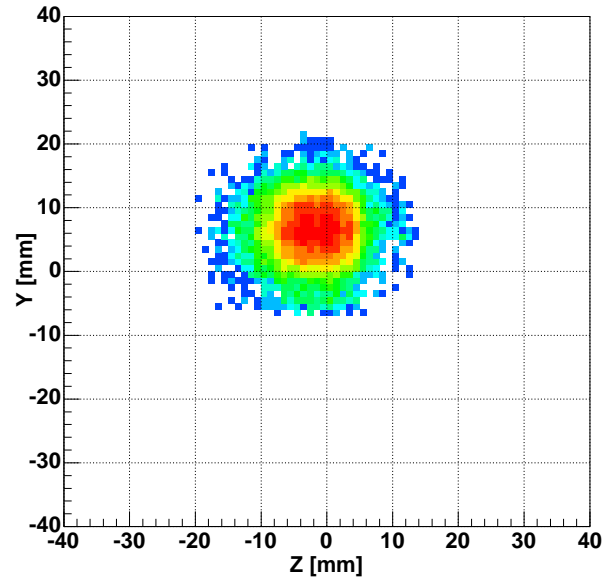


Fig. 7: Image of the target

With the two dimensional position information from both detectors it is possible to reconstruct an image of the target. Figure 7 shows the Y and Z (along the beam) coordinates of the intersection of a track and the Y - Z plane at the X coordinate of the nominal target point. Along the beam the target is $8.8\ \text{mm}$ long (FWHM) while in Y direction the width is $8.4\ \text{mm}$.

References:

- [1] R. Schleichert et al., "A Self-Triggering Silicon-Tracking Telescope for Spectator Proton Detection", IEEE Trans. Nucl. Sci., vol. 50, no. 3, pp. 301-306, 2003
- [2] SRIM - The Stopping and Range of Ions in Matter, Version 2000.24, <http://www.srim.org>

¹ High Energy Physics Department, PNPI, Gatchina, Russia
² Institute of Nuclear and Hadron Physics, Forschungszentrum Rossendorf
³ Laboratory for Nuclear Problems, JINR, Dubna, Russia